Submitted to ApJL September 16; accepted February 2
Preprint typeset using LaTeX style emulateapj

COSMOLOGICAL CONSTRAINTS FROM CURRENT CMB AND SN 1A DATA: A BRUTE FORCE 8 PARAMETER ANALYSIS

Max Tegmark [a,b]

[a]Institute for Advanced Study, Princeton, NJ 08540; max@ias.edu
[b]Hubble Fellow

Submitted to ApJL September 16; accepted February 2

ABSTRACT

We describe constraints on a "standard" 8 parameter open cold dark matter (CDM) model from the most recent CMB and SN1a data. Our parameters are the densities of CDM, baryons, vacuum energy and curvature, the reionization optical depth, and the normalization and tilt for both scalar and tensor fluctuations. We find that although the possibility of reionization and gravity waves substantially weakens the constraints on CDM and baryon density, tilt, Hubble constant and curvature, allowing *e.g.* a closed Universe, open models with vanishing cosmological constant are still strongly disfavored.

Subject headings: cosmic microwave background — supernovae: general

1. INTRODUCTION

The currently most popular cosmological model has of order $N = 10$ free parameters. Upcoming CMB experiments hold the potential to measure these parameters with unprecedented accuracy (Jungman *et al.* 1996; Bond *et al.* 1997; Zaldarriaga *et al.* 1997; Efstathiou & Bond 1998), especially when combined with galaxy redshift surveys (Eisenstein *et al.* 1998) and supernovae 1a (SN 1a) observations (White 1998; Tegmark *et al.* 1998). However, these papers have also demonstrated the importance of fitting for all N parameters jointly, revealing subtle degeneracies by exploring the full N-dimensional parameter space. For this reason, there has been a persistent drive towards larger N when analyzing data. The first analyses based on COBE DMR used $N = 2$ parameters, the CMB quadrupole normalization Q and the scalar tilt n_s of the power spectrum (*e.g.*, Smoot *et al.* 1992; Gorski *et al.* 1994; Bond 1995; Bunn & Sugiyama 1995; Tegmark & Bunn 1995). Since then, many dozens of papers have extended this to incorporate more data and parameters, recent work including Bunn & White (1997); de Bernardis *et al.* (1997); Ratra *et al.* (1998); Hancock *et al.* (1998); Lesgourges *et al.* (1998); Bartlett *et al.* (1998); Webster *et al.* (1998); Lineweaver & Barbosa (1998ab); White (1998); Bond & Jaffe (1998); Gawiser & Silk (1998), and Contaldi *et al.* (1998). The most ambitious analysis to date is that of Lineweaver (1998 – hereafter L98), jointly varying $N = 6$ parameters: n_s, Q, the Hubble constant h and the relative densities Ω_{cdm}, Ω_b and Ω_Λ of CDM, baryons and vacuum energy.

A realistic minimal cosmological model should include all physically well-motivated parameters. Yet even the heroic L98 analysis lacks three: gravity-wave (tensor) fluctuations, parametrized by a relative quadrupole normalization r and a tilt n_t, and the optical depth τ from reionization. In an inflationary context, gravity waves are just as natural as deviations from $n_s = 1$, and we know that $\tau > 0$ since the Universe was reionized before $z = 5$. It is therefore timely to extend this drive towards larger N by analyzing this "minimal" 9-parameter model space. That is the purpose of the present *Letter*.

2. METHOD

In principle, such an analysis is straightforward: compute the theoretical CMB power spectrum C_ℓ with the CMBfast software (Seljak & Zaldarriaga 1996) at a fine grid of points in the N-dimensional parameter space and make χ^2-fits to the available power spectrum measurements in Figure 1. In practice, this is quite tedious. With M grid points in each dimension, M^N power spectra must be computed. Lineweaver's impressive $N = 6$ analysis involved running CMBfast millions of times, corresponding to years of workstation CPU time, and with $M \sim 20$ as in L98, the amount of work grows by more than an order of magnitude for each additional parameter. Fortunately, the underlying physics (see *e.g.* Hu *et al.* 1997 for a review) allows numerical simplifications as described below.

2.1. *Parameter space*

We choose our 9-dimensional parameter vector to be $\mathbf{p} \equiv (\omega_{cdm}, \omega_b, \tau, h, \Omega_k, n_s, n_t, Q, r)$, where the physical densities $\omega_i \equiv h^2\Omega_i$, $i = cdm, b$. The advantage of this parametrization (see Bond *et al.* 1997; Eisenstein *et al.* 1998) will become clear in §2.3. Ω_k is the spatial curvature, so $\Omega_\Lambda = 1-\Omega_k-\Omega_{cdm}-\Omega_b = 1-\Omega_k-(\omega_{cdm}+\omega_b)/h^2$.

We choose our grid to cover the following parameter ranges: $0.02 \le \omega_{cdm} \le 0.8$, $0.003 \le \omega_b \le 0.13$, $0 \le \tau \le 0.8$, $0.2 \le h \le 1.3$, $0 \le \Omega_k \le 0.9$, $0.5 \le n_s \le 1.6$, $0.24 \le n_t \le 1$. This extends the L98 ranges somewhat, since L98 reported high likelihoods near certain grid boundaries. To avoid prohibitively large M, we use a roughly logarithmic grid spacing for ω_{cdm}, ω_b and h, a linear grid spacing for Ω_k, a hybrid for n_s, n_t, τ and no grid at all for the normalization factors Q and r.

Although a fairly fine grid is desirable for the likelihood analysis presented in Section 3, we find that we can attain sufficient accuracy by running CMBfast on a coarser grid and then interpolating the multipoles C_ℓ onto the fine grid. To prevent the resulting model file from exceeding 9 gigabytes in size, we also use an adaptive mesh approach, complementing the global grid with a finer subgrid in the most favored regions of parameter space.

2.2. *Separating scalars and tensors*

If we were to run CMBfast in the standard way, computing scalar and tensor fluctuations simultaneously, we would have to explore an 8-dimensional model grid since only Q drops out as an overall normalization factor. Instead, we compute the scalar fluctuations C_ℓ^{scalar} and the tensor fluctuations C_ℓ^{tensor} separately, normalize them to both have a quadrupole of unity, and compute the combined power spectrum as

$$C_\ell = Q^2 \left[C_\ell^{scalar} + rC_\ell^{tensor}\right]. \qquad (1)$$

We therefore only need to compute two 6-dimensional grids with CMBfast, one over $(\omega_{cdm}, \omega_b, \tau, h, \Omega_k, n_s)$ and the other over $(\omega_{cdm}, \omega_b, \tau, h, \Omega_k, n_t)$.

In addition, we reduce the dimensionality of our parameter space to 8 by imposing the consistency relation (Liddle & Lyth 1992)

$$r = -7n_t. \qquad (2)$$

It holds in all monomial inflation models satisfying the slow-roll conditions (the 2^{nd} relation $n_t = n_s - 1$ holds only for a small subclass). We do this merely because it is well-motivated and reduces error bars – it does not accelerate our calculations.

2.3. *Separating small and large scales*

The multipole moments C_ℓ for $\ell \ll 100$ correspond to fluctuations on scales outside the horizon at recombination. This makes them almost independent of the causal microphysics that create the familiar acoustic peaks, *i.e.*, independent of ω_{cdm} and ω_b. We therefore compute the power spectrum for $\ell \leq 100$ with the fine grid restricted to (τ, h, Ω_k, n_s) or (τ, h, Ω_k, n_t), using only an ultra-course three-point grid for ω_{cdm} and ω_b to pick up weak residual effects aliased down from larger ℓ. We then fill in the rest of the ω_{cdm}- and ω_b-values by interpolation.

For the remaining (high ℓ) part of the power spectrum, more radical simplifications can be made. First of all, the effect of reionization is merely an overall suppression of C_ℓ by a constant factor $e^{-2\tau}$ on these small scales. Second, the effect of changing both Ω_k and h (and implicitly Ω_Λ) is merely to shift the power spectrum sideways. This is because the acoustic oscillations at $z \gtrsim 1000$ depend only on ω_{cdm} and ω_b, and the geometric projection of these fixed length scales onto angular scales θ in the sky obeys $\theta(\Omega_m, \Omega_\Lambda, h) \propto 1/d_A(\Omega_m, \Omega_\Lambda, z_{lss})$. Here d_A is the luminosity distance

$$d_A = (1+z_{lss})\frac{S(\kappa I)}{H_0\kappa}, \quad \kappa \equiv \sqrt{|1-\Omega_m-\Omega_\Lambda|}, \qquad (3)$$

$$I = \int_0^{z_{lss}} \frac{dz'}{[(1+z')^2(1+\Omega_m z') - z'(2+z')\Omega_\Lambda]^{1/2}}, \qquad (4)$$

where $S(x) \equiv \sinh x$, x and $\sin x$ for open $(\Omega_m + \Omega_\Lambda < 1)$, flat $(\Omega_m + \Omega_\Lambda = 1)$ and closed $(\Omega_m + \Omega_\Lambda > 1)$ universes, respectively. We compute z_{lss}, the effective redshift of the last scattering surface, using the fit in Appendix E of Hu & Sugiyama (1996).

Ω_m and Ω_Λ also modify the late integrated Sachs-Wolfe effect, but this is important only for $\ell \lesssim 30$ (Eisenstein *et al.* 1998). The only other effect is a small correction due to gravitational lensing (Metcalf & Silk 1998; Stompor & Efstathiou 1998), which we ignore here because of the large error bars on current small-scale data. To map the model $(\Omega_m^*, \Omega_\Lambda^*, h^*)$ into the model $(\Omega_m, \Omega_\Lambda, h)$, one thus shifts its high ℓ power spectrum to the right by an ℓ-factor of $\theta(\Omega_m^*, \Omega_\Lambda^*, h^*)/\theta(\Omega_m, \Omega_\Lambda, h)$.

We therefore adopt the following procedure. We compute the $\ell \geq 100$ part of the power spectrum for a 3-dimensional grid over $(\omega_{cdm}, \omega_b, n_s)$ or $(\omega_{cdm}, \omega_b, n_t)$. We extend this grid to include h and Ω_k by shifting it sideways as described, then merge it with the low ℓ grid by adjusting its normalization to match at $\ell = 100$. In addition to reducing the dimensionality of the grids computed with CMBfast, this approach has the advantage that only flat models need to be run for the high grid, with the (much slower) computations involving curvature and reionization only being required up to $\ell = 100$.

Extensive tests show that these approximations typically reproduce the power spectrum to about 5% accuracy for generic models, *i.e.*, substantially better than the current measurement errors. As data quality improves, the errors introduced by the above-mentioned approximation scheme can of course be continuously reduced to zero by refining the (ω_{cdm}, ω_b)-grid for low ℓ and shifting the splicing point upwards from $\ell = 100$.

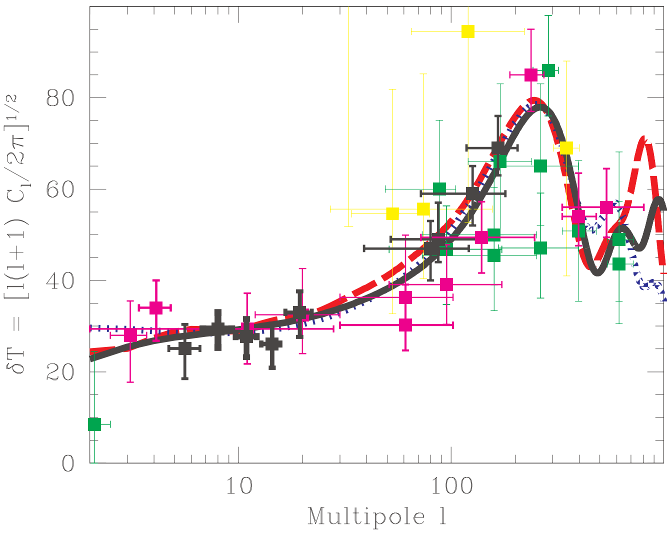

FIG. 1.— Three models (see text) are shown together with the 37 CMB data points, with the line weight and shading emphasizing those with small error bars.

2.4. *Data and likelihoods*

We use the compilation of CMB data and window functions of L98 with the addition of the new QMAP results (Devlin *et al.* 1998; Herbig *et al.* 1998; de Oliveira-Costa *et al.* 1998), from which we use the two points combining both flights. The 37 band powers are shown in Figure 1. We compute our likelihood function as $L(\mathbf{p}) \propto e^{-\chi^2/2}$, where the χ^2 fit of the data to $C_\ell(\mathbf{p})$ is computed as in L98. This procedure has a number of deficiencies as we will now describe. The probability distributions for the measurements are not Gaussian. In addition, the error bars for all experiments include a sample variance term which depends on $\mathbf{p}$, and this dependence is rarely included explicitly in quoted measurement results. A better (offset log-normal) approximation for the band-power likelihood is given by Bond *et al.* (1998), but for most experiments, the additional parameter that it requires has unfortunately not been computed yet. Finally, if the likelihood function $L(\mathbf{p})$ is a multivariate Gaussian, then one can show that marginalizing (integrating) over a subset of parameters is equivalent (up to an irrelevant normalization factor) to maximizing over them. We will follow L98 in doing the latter, since it is both simpler and avoids the unpleasant ambiguities of choosing a Bayesian prior — alas, with a uniform prior, our 9-dimensional normalization integral would not even converge. As we will see, our L is in fact highly non-Gaussian in some directions, which means that our confidence limits must be taken with a grain of salt. They also depend on the choice of Bayesian prior, as described in §3.2.

However, to put these statistical issues in perspective, this author feels that an even more pressing challenge will be to test the data sets for systematic errors, *e.g.*, by comparing them pairwise where they overlap in sky coverage and angular resolution (Knox *et al.* 1998; Tegmark 1998).

3. RESULTS AND CONCLUSIONS

3.1. *Best fit*

The best fit model is shown in Figure 1, and gives $\chi^2 = 22.9$. The probability of obtaining such a low χ^2-value with $37-8=29$ effective degrees of freedom is about 22%, so although CMB experimentalists have occasionally been accused of underestimating their error bars, we are closer to the opposite situation here.

It is noteworthy that despite our large parameter space, the best fit model $\tau = r = 0$, $\Omega_k = 0.3$, $h^2\Omega_{cdm} = 0.2$, $h^2\Omega_b = 0.025$, $h = 0.5$ and $n_s = 1.0$ (solid line in Figure 1) is comparatively boring, preferring neither reionization, gravity waves nor tilt and giving rather conventional values of $h^2\Omega_b$ and h. Much more exotic models are also allowed, however. If we restrict the parameter search to flat models ($\Omega_k = 0$), the best fit is $\tau = 0.5$, $r = 0$, $h^2\Omega_{cdm} = 0.35$, $h^2\Omega_b = 0.04$, $h = 0.4$ and $n_s = 1.4$, dashed in Figure 1, where the high acoustic peaks that would be caused by the strong blue-tilting and the high baryon density are tempered by very early reionization. If we restrict ourselves to inflationary "vanilla" models with $\tau = \Omega_k = r = 0$ and $n_s = 1$, the best fit is $h^2\Omega_{cdm} = 0.1$, $h^2\Omega_b = 0.02$ and $h = 0.4$, dotted in Figure 1.

3.2. *Single-parameter constraints*

Constraints on individual parameters are shown in Figure 2 and Table 1, interpolating their marginal distributions. Gravity waves are seen to be generally disfavored, with the maximum-likelihood value $n_t = 0$ corresponding to $r = 0$, no gravity waves at all. The best fitting models all fail to quite match the low COBE DMR quadrupole, and tensors merely make this worse by adding additional large scale power. Reionization is also mildly disfavored, for the same reason — increasing τ and simultaneously increasing Q by a factor e^τ causes mainly a net rise at small ℓ. However, this feature is softer than that of gravity waves, so as illustrated in Figure 1, it can be largely offset by increasing n_s, ω_b and ω_{cdm}. The result is that there are no relevant constraints on τ: not even the extreme case $\tau = 0.8$ can be ruled out from our CMB data.

The thin lines show the constraints assuming $\tau = r = 0$, as in L98, and agree well with the L98 results considering that these did not include QMAP. However, the heavy lines show that including r and τ substantially weakens these bounds. Gravity waves and reionization soften the upper limits on n_s, ω_{cdm} and ω_b since they can lower the acoustic peaks given COBE-normalization on large scales.

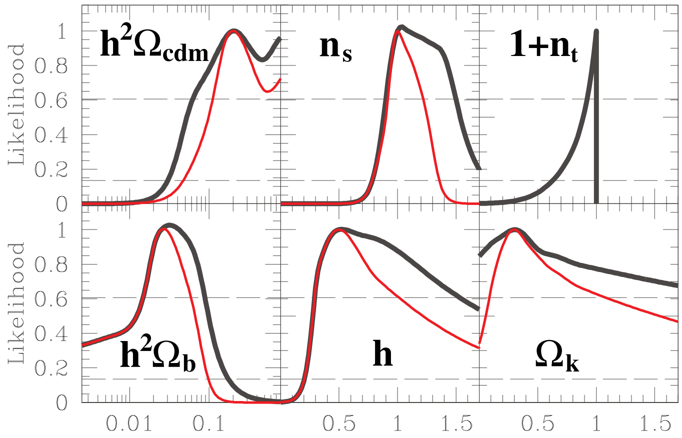

FIG. 2.— Heavy lines show likelihoods for individual parameters marginalized over all others. Thin lines show the stronger constraints resulting from assuming neither reionization nor gravity waves. If the likelihood were Gaussian, the 68% and 95% confidence limits would lie where the curves cross the two dashed lines (see Table 1).

We have followed L98 in using a uniform prior, truncated outside the explored parameter range. Whereas L98 limited this range to values considered reasonable, we have attempted to quantify what CMB alone can say, extending the range far enough for the likelihood to become small. Figure 2 shows that this was achieved for all parameters except ω_{cdm}, where our exclusion of (quite unreasonable) values $h^2\Omega_{cdm} > 0.8$ matters. For a full Bayesian analysis, our CMB likelihood function should be multiplied by the likelihood functions from all other relevant astrophysical measurements.

3.3. *Constraints on the acceleration of the Universe*

The above-mentioned fact that Ω_k and h (and implicitly Ω_Λ) both shift the high ℓ power spectrum sideways make them rather degenerate. To better understand the constraints on these quantities, we therefore plot them in the two-dimensional $\Omega_m - \Omega_\Lambda$ plane (Figure 3), where $\Omega_m \equiv \Omega_{cdm} + \Omega_b$. Our results for $\tau = r = 0$ agree well with those of L98 when considering that (a) our analysis includes QMAP and (b) we have plotted our 68% and 95% confidence contours at $\Delta\chi^2 = 2.29$ and 6.18, respectively, since they are two-dimensional, as in Press *et al.* (1992) §15.6, whereas L98 used $\Delta\chi^2 = 1$ and 4. Unfortunately, CMBfast cannot currently handle closed ($\Omega_k < 0$) models (White & Scott 1996). As L98 points out, the likelihood is already decreasing as one approaches the diagonal $\Omega_k = 0$ line (dotted) from the lower left, so we have simply extended our likelihood function to $\Omega_k < 0$ by extrapolation. When dropping the $\tau = r = 0$ assumption, however, this is no longer true, and the upper right (light grey) region of the $\Omega_m - \Omega_\Lambda$ plane is no longer excluded.

Figure 3 also shows that the constraints at the lower left are unaffected by reionization and gravity waves. This asymmetry is easy to understand physically. This region is ruled out because the first acoustic peak is too far to the right, whereas the light grey region had the peak too far to the left. Adding a strong blue-tilt can shift the peak slightly to the right, but never to the left. Figure 1 showed that such a tilted peak could be lowered back to the original height using τ and r, making it fit the data, but τ and r clearly cannot raise a (red-tilted) peak.

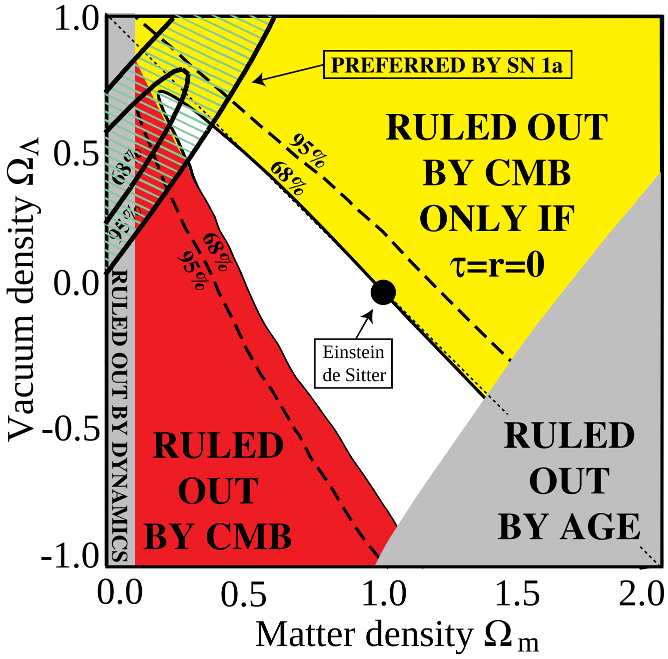

FIG. 3.— Constraints in the $\Omega_m - \Omega_\Lambda$ plane. Apart from our CMB constraints, $\Omega_m < 0.1$ would be inconsistent with the amount of matter observed dynamically. For the age we have simply taken $H_0 t_0 > 0.6$ as a lower limit. The region preferred by SN 1a is that computed by White (1998) from the combined data of the two supernova teams. In addition, gravitational lensing constrains the upper left corner.

The recent constraints from SN 1a are highly complementary to our CMB constraints. Figure 3 shows the SN 1a constraints computed by White (1998) in a joint analysis of the published data from the two search teams (Perlmutter *et al.* 1998; Riess *et al.* 1998; Garnavich *et al.* 1998). We see that even including r and τ, the combined CMB and SN 1a data prefer $\Omega_\Lambda \gtrsim 0.5$, with a vanishing cosmological constant strongly disfavored. The conclusion that $\Omega_m \lesssim 0.5$ does *not* survive the inclusion of r and τ, however, and we cannot rule out the possibility that the Universe is closed.

3.4. *Outlook*

In conclusion, we have performed a brute force 8 parameter fit of cosmological models to the currently available CMB data and compared this with SN 1a constraints. We found that although the inclusion of reionization and gravity waves weakened many bounds, interesting constraints remain on *e.g.* Ω_Λ. Quoted error bars on parameters have grown steadily since the first COBE results, as more parameters have been included in the analysis. Since we have now extended our parameter space to essentially the full "minimal cosmological model", the error bars might be as large in this *Letter* as they will ever get. From now on, the rapid improvement in data quality will hopefully decrease them faster than they are diluted by the addition of further parameters, ushering us into the era of precision cosmology.

Table 1 – Maximum-likelihood values and 68% confidence limits

	6 Parameters			8 Parameters		
Quantity	Min	Best	Max	Min	Best	Max
$h^2\Omega_{cdm}$	.11	.20	–	.063	.20	–
$h^2\Omega_b$	.015	.027	.061	.015	.032	.087
h	.29	.49	1.01	.29	.49	1.50
Ω_k	.09	.31	1.05	–	.31	–
n_s	.92	.99	1.22	.92	1.04	1.51
n_t				−0.08	0.0	0.0
r				0.0	0.0	.56

The author wishes to thank Charley Lineweaver for kindly providing his compilation of CMB data, and him and Robert Caldwell, Angélica de Oliveira-Costa, Daniel Eisenstein, Wayne Hu, Douglas Scott and Paul Steinhardt for useful discussions. Support for this work was provided by NASA though grant NAG5-6034 and Hubble Fellowship HF-01084.01-96A from STScI, operated by AURA, Inc. under NASA contract NAS5-26555.

REFERENCES

Bartlett, J. *et al.* 1998, astro-ph/9804158
de Bernardis, P. *et al.* 1997, *ApJ*, **480**, 1
Bond, J. R. 1995, *Phys. Rev. Lett.*, **74**, 4369
Bond, J. R., Efstathiou, G., & Tegmark, M. 1997, *MNRAS*, **291**, L33
Bond, J. R., & Jaffe, A. H. 1998, astro-ph/9809043
Bond, J. R., Jaffe, A. H., & Knox, L. E. 1998, astro-ph/9808264
Bunn, E. F., & Sugiyama, N. 1995, *ApJ*, **446**, 49
Bunn, E. F., & White, M. 1997, *ApJ*, **480**, 6
Contaldi, C., Hindmarsh, M., & Magueijo, J. 1998, astro-ph/9809053
de Oliveira-Costa, A. *et al.* 1998, *ApJL*, **509**, L77
Devlin, M. *et al.* 1998, *ApJL*, **509**, L69
Efstathiou, G., & Bond, J. R. 1998, astro-ph/9807103
Eisenstein, D. J., Hu, W., & Tegmark M 1998, astro-ph/9807130
Garnavich, P. M. *et al.* 1998, *ApJ*, **509**, 74
Gawiser, E., & Silk, J. 1998, *Science*, **280**, 1405
Gorski, K. M. *et al.* 1994, *ApJL*, **430**, L89
Hancock, S. *et al.* 1998, *MNRAS*, **294**, L1
Herbig, T. *et al.* 1998, *ApJL*, **509**, L73
Hu, W., & Sugiyama, N. 1996, *ApJ*, **471**, 572
Hu, W., Sugiyama, N., & Silk, J. 1997, *Nature*, **386**, 37
Jungman, G., Kamionkowski, M., Kosowsky, A., & Spergel, D. N. 1996, *Phys. Rev. D*, **54**, 1332
Knox, L. *et al.* 1998, *Phys. Rev. D*, **58**, 083004
Lesgourgues, J. *et al.* 1998, astro-ph/9807019
Liddle, A. R., & Lyth, D. H. 1992, *Phys. Lett. B*, **291**, 391
Lineweaver, C. H. 1998, *ApJL*, **505**, L69 ("L98")
Lineweaver, C. H., & Barbosa, D. 1998a, *A&A*, **329**, 799
Lineweaver, C. H., & Barbosa, D. 1998b, *ApJ*, **496**, 624
Metcalf, R. B., & Silk, J. 1998, *ApJ*, **489**, 1
Perlmutter, S. *et al.* 1998, *Nature*, **391**, 51
Press, W. H. *et al.* 1992, *Numerical Recipes, 2nd ed.* (Cambridge Univ. Press: Cambridge)
Ratra, B. *et al.* 1998, astro-ph/9807298
Riess, A. G. *et al.* 1998, *Astron. J.*, **116**, 1009
Seljak, U., & Zaldarriaga, M. 1996, *ApJ*, **469**, 437
Smoot, G. F. *et al.* 1992, *ApJ*, **396**, L1
Stompor, R., & Efstathiou, G. 1998, astro-ph/9805294
Tegmark, M. 1998, astro-ph/9809001
Tegmark, M., & Bunn, E. F. 1995, *ApJ*, **455**, 1
Tegmark, M., Eisenstein, D. J., Hu, W., & Kron, R. 1998, astro-ph/9805117
Webster, M. *et al.* 1998, *ApJL*, **509**, L65
White, M. 1998, *ApJ*, **506**, 495
White, M., & Scott, D. 1996, *ApJ*, **459**, 415
Zaldarriaga, M., Spergel, D., & Seljak, U. 1997, *ApJ*, **488**, 1